

- (17) J. W. Brewer, "The bilinear, modal state equations for age-dependent growth control", *ASME J. Dynamic Systems Measurement Control*, Vol. 103, pp. 89-94, June 1981.
- (18) J. W. Brewer, "Population modelling", in "Systems and Control Encyclopedia", pp. 3756-3762, Pergamon Press, Oxford, 1988.
- (19) N. Keyfitz, "Introduction to the Mathematics of Population", Addison-Wesley, London, 1968.
- (20) M. Hubbard and J. W. Brewer, "Pseudo bond graphs of circulating fluids with application to solar heating design", *J. Franklin Inst.*, Vol. 311, No. 6, pp. 339-354, 1981.
- (21) T. Matsumoto, L. O. Chua and M. Komuro, "The double scroll", *IEEE Trans Circuits Systems*, Vol. CAS-32, No. 8, pp. 797-818, Aug. 1985.
- (22) A. H. Jazwinski, "Stochastic Processes and Filtering Theory", Academic Press, San Francisco, 1970.

## Controller Design in the Physical Domain†

by ANDRE SHARON, NEVILLE HOGAN and DAVID E. HARDT

Department of Mechanical Engineering, Laboratory for Manufacturing and Productivity, Massachusetts Institute of Technology, Cambridge, MA 02139, U.S.A.

**ABSTRACT:** "Design in the Physical Domain" is proposed as a means of integrating control systems design with mechanical systems design. This approach facilitates separation of design issues from implementation issues through high-level abstraction, and provides guidance in selecting the proper physical architecture for a given control task. As an example it is shown how this philosophy may lead to alternative robot architectures that are inherently stable and well-suited for high performance end-point control.

### 1. Introduction

Control systems design is generally perceived as the manner in which measurement signals are conditioned and then used to specify input levels applied to actuators. The process is often independent of the mechanical design process, and usually follows it. It is commonly assumed that the mechanical system already exists when the controller design phase is begun. Yet the time at which a mechanical or electro-mechanical design is specified is also the time when many restrictions are inadvertently placed on the controller design. Unfortunately, some characteristics that are considered beneficial from a mechanical design point of view may actually be detrimental from a control point of view.

Consider, for example, the space-shuttle arm. Its low mass is ideal for the application, since the cost of each kilogram of payload is phenomenal. On the other hand, its resulting low stiffness makes it extremely difficult to control.

Similarly, mechanical designers often strive to achieve as much shared functionality as possible. This reduces the number of components required in an assembly, perhaps improving reliability while reducing cost. Incorporating only six actuators (not counting the gripper) into commercial robots demonstrates this philosophy. After all, this is the minimum number required to arbitrarily specify a position and orientation in space. From a mechanical design point of view, there appears to be no reason for adding redundant actuators to the system. Yet, as will be shown in this paper, the use of redundant actuators, properly located, is what makes a macro/micro-manipulator architecture (1-4) inherently more stable and better suited for control than conventional robot architectures. This insight is lost, however, if the controller design is not integrated with the mechanical design.

Consider the most common procedure for designing control systems. First, the

† Portions of this paper have been presented at the IEEE International Conference on Robotics and Automation, and the American Control Conference.

system to be controlled is modeled using one of the established techniques. The equations of motion describing the system are then derived from that model. The next step usually involves linearization and Laplace transformation in order to work in the  $s$ -plane, using the well-known methods of classical control. If modern control is used, the system gains may be determined in the time domain. Both of these approaches are very useful in that they provide a mathematical methodology for designing controllers. However, they assume a given system and do not provide any guidance in designing that system in the first place. Furthermore, insight into the limitations of the physical system may be obscured when working in the Laplace domain ( $s$ -plane), or when using the mathematical theory of modern control.

## II. Physical Equivalence

We suggest that because control systems design begins with mechanical systems design, a unified approach should be taken. The postulate of *physical equivalence* can provide a link between the two disciplines. It states that for every controlled physical system there exists a physical system with no controller whose dynamic-interaction behavior is identical. Hogan (5) further conjectures (without proof) that "it is impossible to devise a controller which will cause a physical system to present an apparent behavior to its environment which is distinguishable from that of a purely physical system". Thus, in our view, all a controller can do is alter the behavior of one physical system such that it emulates the behavior of another physical system. The value of this conjecture is that if a controlled system truly emulates another physical system whose behavior is known, then the complete controlled system can be characterized regardless of the details of how the controller accomplishes that task. For example, if a controlled system truly emulates a mass-spring damper system, then it can be concluded that the system is stable, regardless of the implementation (6).

There are many possible control implementations that might make a physical system emulate a mass-spring-damper system. Thus, describing a controlled system as an equivalent physical system is a higher-level abstraction of the control system's action. It is a many-to-one mapping analogous to *abstraction by specification* in computer languages. In designing complex computer programs, abstraction is heavily used as a means of focusing on the task of the program without being distracted by an unmanageable level of detail. Similarly, the control systems designer can use physical equivalence as a means of abstraction in developing controllers. Though it may initially seem counter-intuitive, the abstraction of physical equivalence facilitates separation of design issues from implementation issues. It also facilitates controller design in the physical domain.

## III. Design in the Physical Domain

Design in the physical domain (1) is proposed as a means of unifying control systems design with mechanical systems design by preserving physical insight and providing guidance in the selection of the proper physical architecture for control. Although this approach is still in its infancy and a formal procedural methodology

has yet to be developed, we will show in this paper how it can be used to tie together several mechanical and control-related issues.

The approach is based on the concept of physical equivalence described above. It is also based on the following key postulate made by the authors. Given ideal actuators and sensors:

any physical system can be made to emulate the dynamic behavior of any other physical system, provided that *ideal* actuators and sensors can be placed at any point in the system.

Since the concept of a "physical system" is central to the development of this paper, a clarification of what we mean by a "physical system" is warranted. While all systems may be "physical" (in the sense that they obey the laws of physics) at one level or another, at the operational level (the level of interest) they may not present a physical behavior. A computer, for example, is certainly a physical device at the hardware level. However, at the operational level (information processing in this case) the system behavior is not constrained by some of the more important physical laws such as energy conservation, etc. Indeed, aside from the requirement that its output may not precede its input in time, any dynamic functional relationship may be implemented. For example, it is trivial to implement in software a controller that commands a mass to change its velocity instantaneously. Thus, the controller presents an operational behavior that is non-physical, even though at a lower level the computer is certainly a physical device. This "non-physical" controller, however, will *not* be capable of imposing such a "non-physical" behavior on the mass. Rather, the mass will respond with a finite acceleration, and the complete controlled system (mass plus controller) will present a behavior that is completely consistent with physical constraints; this is the essence of the postulate of *physical equivalence*.

Ideal actuators and sensors were introduced to serve as a link between the physical domain and the information processing domain, and are defined as follows.

An *ideal actuator* is a fictitious device which generates a force† in strict proportion to a control signal at all frequencies. It is the "controlled source" commonly used in circuit theory and physical system modeling.

An *ideal sensor* is a fictitious device which generates a signal (such as voltage, a digital word, etc.) in strict proportion to a physical variable (such as force, velocity, position, etc.) at all frequencies.

Since in reality all actuators and sensors exhibit some dynamics of their own, a controlled physical system cannot perfectly emulate a desired system. Nevertheless, it can closely approximate the desired behavior for a certain frequency range. Also, actuators and sensors cannot be arbitrarily placed anywhere in a real system. Thus, the "art" of designing controllers in the physical domain consists of selecting a target physical system that can be approximated with achievable actuation and sensing, and wisely locating available actuators and sensors.

† In general, an ideal actuator may generate either an effort (such as force, voltage, etc.) or a flow (such as velocity, current, fluid-flow, etc.).

Location of actuators and sensors, in our view, is the most important and influential factor in achieving a desired control system. Yet, it is often considered to be part of the mechanical or electromechanical design phase. It is therefore very advantageous that the mechanical design phase be an integral part of the control system design phase.

To facilitate the synthesis of new physical architectures using Design in the Physical Domain, and to provide guidance in locating actuators and sensors we use the following equivalences as building blocks.<sup>†</sup>

If an ideal actuator and corresponding ideal sensor are acting on the same point (collocated control) in a purely inertial system, then:

1. Negative position feedback is equivalent to a spring action.
2. Negative velocity feedback is equivalent to a damping action.
3. Negative force feedback is equivalent to decreasing inertia.
4. Positive force feedback is equivalent to increasing inertia.

Designing a controller "in the physical domain" consists of the following steps:

1. Designing the controller structure in the physical domain by first assuming that actuators and sensors can be placed anywhere in the system.
2. Modifying the controller structure such that unfeasible actuation and sensing is eliminated.
3. Fine tuning the controller parameters using common control techniques ( $s$ -plane, optimization theory, simulation, etc.).

Designing the controller structure includes decisions such as the proper target physical system for the task, the proper states to measure (sensor location), and the proper states to actuate (actuator location). This should (naturally) be done in the physical domain where the most physical insight is available. In this way a great deal is automatically specified about the mechanical design in the process of designing the controller structure. It is in this regard that the method we propose differs most from the more conventional controller design techniques.

Once the structure of the control system has been designed, the system parameters (gains, etc.) can be fine-tuned using any of the common control techniques as necessary. Thus, controller design in the physical domain is not presented as an alternative to classical or modern control. Rather, it is presented as a means of unifying existing control methodologies with mechanical design through the higher-level abstraction of physical equivalence.

#### IV. Application to Robot Control

In order to illustrate the distinction between controller design in the physical domain and the more conventional approaches, the design of an impedance-

<sup>†</sup> As an aside, effective use of Design in the Physical Domain may require a more extensive "library" of physical equivalents. Methods to identify equivalent physical systems have been explored in (7).

controlled robot will be considered. Complete details of the work described below are presented in (3). For background, a brief review of impedance control follows.

Impedance control has been proposed (5) as a general framework for controlling manipulation. To date it has been shown to be effective in many robot applications including both contact and non-contact tasks (8, 9). Force, position, and velocity feedback are viewed as means of modulating the apparent impedance of the system rather than as sources of error signals to be suppressed by a regulator attempting to track a given input. Modulating the end-point impedance of the robot (that seen by the environment) facilitates interaction with various environments. Increasing the range over which the robot impedance can be modulated also broadens the class of environments that the robot can successfully interact with. This is very difficult to achieve using conventional robot architectures.

Consider the simple lumped-parameter, one-axis model of a robot shown unconstrained in Fig. 1(a) and interacting with a rigid environment through a force transducer in Fig. 1(b). The robot is actuated ( $F$ ) at the base as are most commercially available robots. The joint dynamics are lumped into  $B_1$  and  $M_1$ , while the structural dynamics are lumped into  $B_2$ ,  $K$ ,  $M_2$ . The force transducer dynamics are denoted by  $K_t$  and  $B_t$ . An important aspect of impedance control is the desired target impedance. Assume the end-point of the robot ( $M_2$ ) is to exhibit the impedance of a mass-spring-damper system with parameters  $M_a$ ,  $B_a$ ,  $K_a$ .

To facilitate quantitative evaluation of impedance controllers and comparison with alternative approaches, we concentrate in this paper on end-point position and force control. The performance of position and force controllers can readily be measured in terms of bandwidth, settling time, overshoot, etc. Thus, the goal is to achieve high-performance control of end-point position ( $X_2$ ) in the system of Fig. 1(a), and high performance control of the force exerted on the environment (which will be assumed equal to the force in the elastic element of the force sensor,  $F_t$ ) in the system of Fig. 1(b).

#### IV.1. The classical control approach

Consider two simple controllers, using end-point position control ( $F = -GX_2$ ) in the system of Fig. 1(a) and end-point force control ( $F = -GF_t$ ) in the system of Fig. 1(b). Taking the classical control approach, the equations describing the two systems may be derived (see Appendix), and root loci (see Fig. 2) obtained.<sup>†</sup> This parameter values used in these calculations are not important in the context of this discussion. They characterize the hardware described in this paper and can be found in Ref. (1). Examining the root loci, it is observed that as the gain is increased, both systems become unstable and no gain can be found where the controller gives an acceptable performance. This is characteristic of non-collocated control, where there is a dynamic system separating the actuator from the sensor (10-12).

It must then be decided whether to measure more states, and how to condition those measurements in order to avoid instability. With the proper control algorithm,

<sup>†</sup> Note that to highlight the salient features of the root locus [e.g. Fig. 2(b)], the horizontal and vertical axes are different.

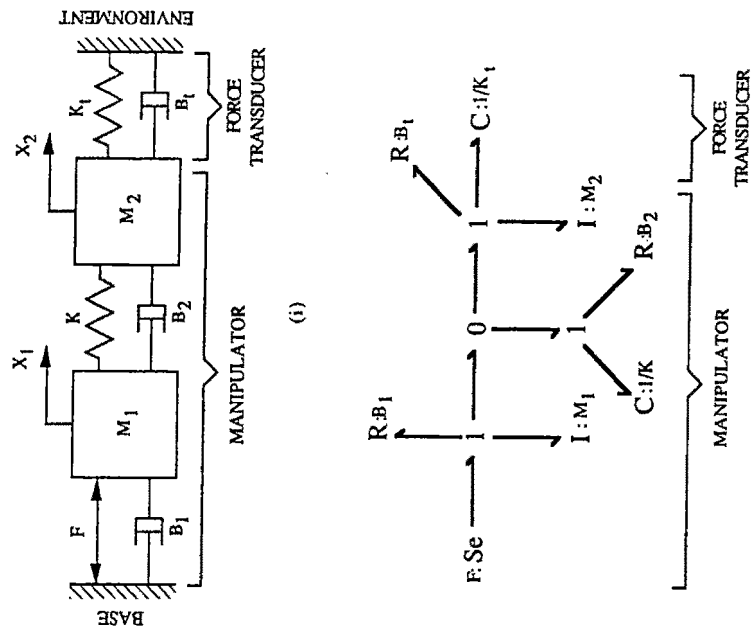


FIG. 1. (a) Model of a one-axis manipulator. (i) Schematic diagram. (ii) Bond graph.

the effect of the undesirable dynamics can be cancelled, and end-point control at bandwidths higher than the structural modes of the system can be achieved (11). However, this requires a very accurate dynamic model of the system, and hence may not be robust. This is confirmed by the fact that the end-point position and force control performance levels achieved to date with conventional robot architectures are very low. These architectures are inherently ill-suited for end-point control.

IV.2. The physical domain approach

Consider now, in contrast, how the system might be designed in the physical domain using physical systems theory. Though it is not specifically represented in the models of Fig. 1, in the actual system there is a fundamental limitation caused by the propagation delay in the structure (the time taken for an input event at one end of the structure to propagate to the other end) (7, 11). Therefore, referring to

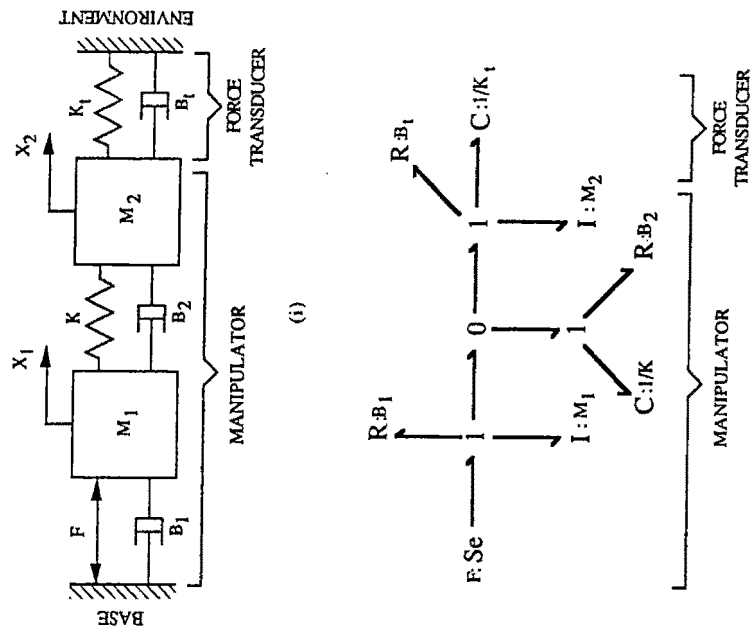


FIG. 1. (b) Model of a one-axis manipulator coupled to a rigid environment. (i) Schematic diagram. (ii) Bond graph.

Fig. 1, it is impossible to change the behavior of  $M_2$  at high frequencies if the actuator is not acting directly on  $M_2$ . Thus, design in the physical domain is begun with the assumption that actuators and sensors can be placed anywhere in the system.

In order to avoid propagation delays, we first attempted to place an actuator between  $M_2$  and ground. This gives rise to a situation of collocated control, thus, according to the equivalences given in the previous section, position, velocity, and force feedback may be used to specify the behavior of  $M_2$ . While placing an actuator between  $M_2$  and ground may at first seem impractical, it can be accomplished by strategically placing several actuators throughout the workspace to which the robot would attach itself. This, in fact, represents a modified version of the focal support concept (13, 14), in which the passive supports are replaced by active ones. Thus, it is seen how this design approach can suggest an alternative physical architecture that is better suited for end-point control.

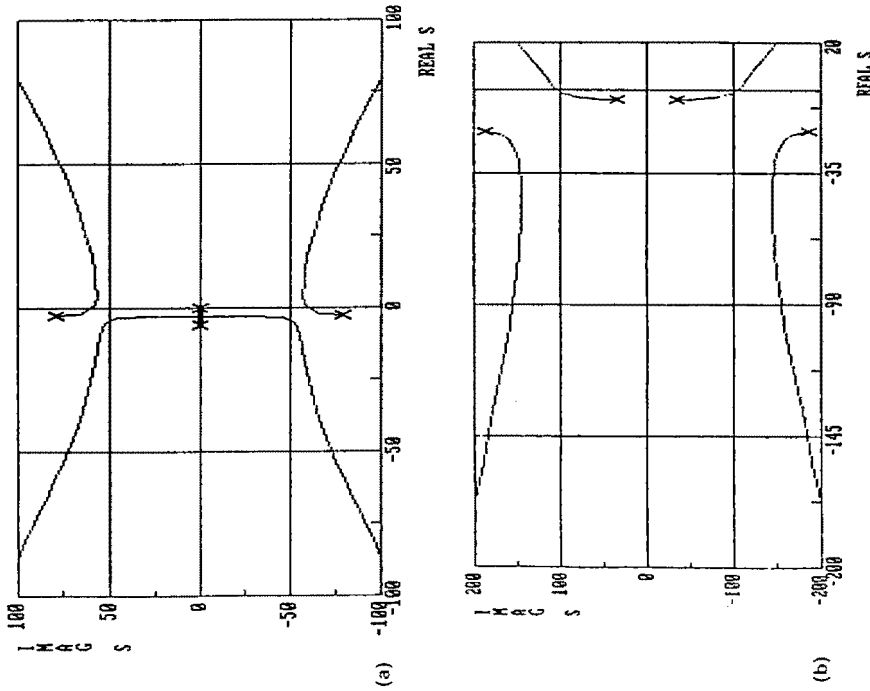


FIG. 2. (a) Root locus of end-point position control ( $F = -GX_2$ ) on a one-axis manipulator. (b) Root locus of force control ( $F = -GF_1$ ) on a one-axis manipulator (a zero at far left not shown).

Local supports may or may not be practical depending on how cluttered the workspace is and the level of flexibility desired. If it is decided that actuation on the end-point from ground is impractical, then the next closest scenario may be considered—an actuator which drives the end-point relative to the robot rather than relative to ground. This arrangement is depicted unconstrained in Fig. 3(a) and interacting with the environment in Fig. 3(b). The actuator is denoted by  $f$ , along with some corresponding damping ( $B_1$ ) and inertia ( $M_1$ ) which now becomes the end-point inertia. In fact, this represents a macro/micro-manipulator architecture, consisting of a large (macro) robot carrying a small (micro) high-performance robot (2). Again, though in this case our analysis is *post hoc*, it can be seen (qualitatively) that the physical domain approach can provide a way of

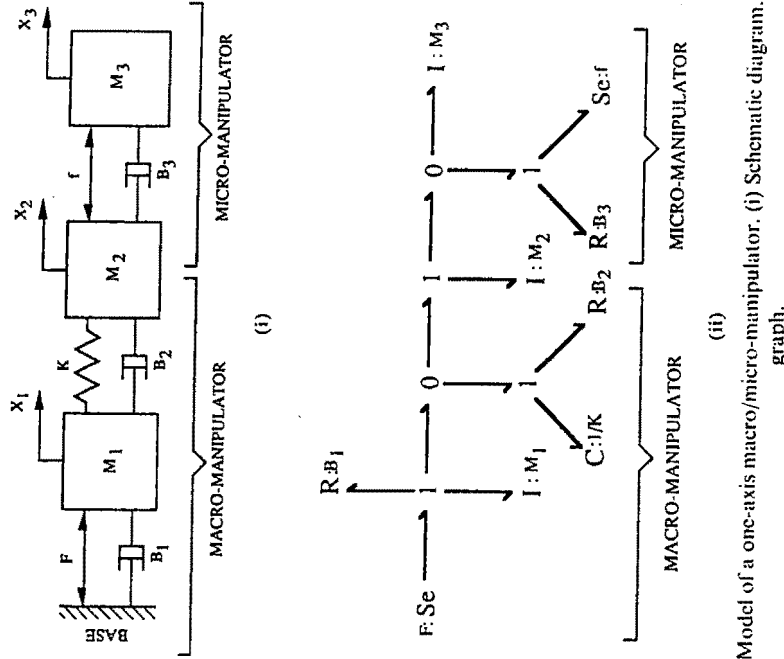


FIG. 3. (a) Model of a one-axis macro/micro-manipulator. (i) Schematic diagram. (ii) Bond graph.

identifying configurations of the mechanical and control system which are better suited to the overall design goal. A more quantitative and formal methodology is clearly needed but has yet to be developed.

While this design process continues to apply to both systems in Fig. 3, for brevity, in the following we will pursue only the constrained (force control) situation. Assuming proportional end-point force control ( $f = -GF_1$ ), the equations describing the system in Fig. 3(b) are derived (see Appendix) and the root locus and Bode plot are obtained (see Figs. 4 and 5). Again, the parameter values can be found in Ref. (1). Examining the root locus and Bode plot, it is observed that the system is stable for all values of the gain parameter,  $G$ , where  $G \in (-\infty, \infty)$ . This is true of the model in Fig. 3(b). Of course a real system would exhibit higher order dynamics and hence would never be stable for all values of  $G$ .

Although not shown, the unconstrained system in Fig. 3(a) is also stable (1). Note that familiar classical control techniques may still be used as tools for analysis and to tune the parameters. However, the design process is done in the physical domain.

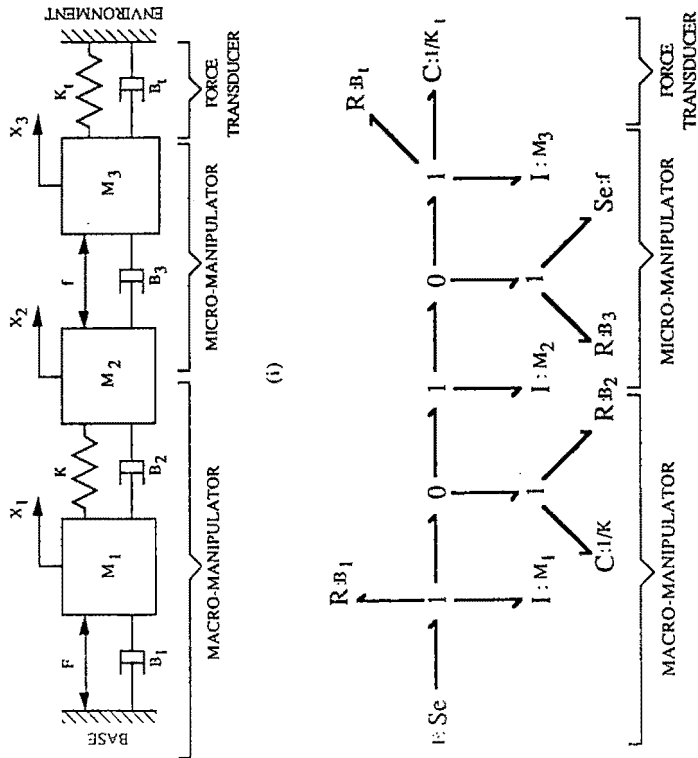


FIG. 3. (b) Model of a one-axis macro/micro-manipulator coupled to a rigid environment. (i) Schematic diagram. (ii) Bond graph.

While this macro/micro-manipulator architecture proves to be inherently stable, further examination of the Bode plot reveals some anti-resonance due to the macro-manipulator's structural dynamics. This undesirable characteristic may be alleviated by attempting to design a compensator using standard techniques of classical control. However, it is not at all clear from the root locus and Bode plot in Figs. 4 and 5 what compensation to use. The root locus and Bode plot contain information regarding stability, natural frequencies, etc., that is very useful in the analysis process, but they do not provide insight into the physical causes of these phenomena, and that is crucial in the design phase. We believe that this dearth of physical insight is typical of all conventional control system design techniques which encourage abstraction away from physical elements. On the other hand, this abstraction to a "mathematical domain" of some sort is extremely effective in providing formal procedural methodologies.

How might this problem be corrected in the physical system? Examining the macro/micro-manipulator model of Fig. 3(b) again, it can be seen that raising the impedance of the macro-manipulator reduces the possibility of the micro-

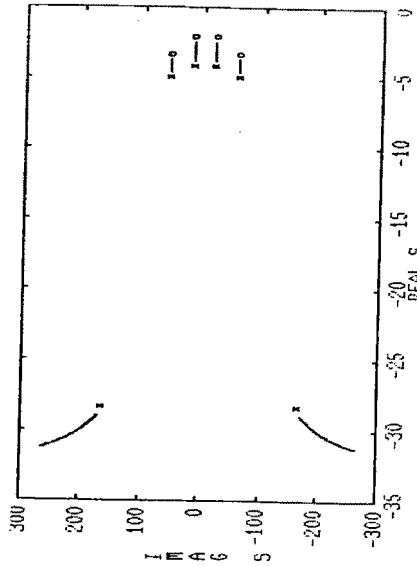


FIG. 4. Root locus of force control ( $J = -KF$ ) on a macro/micro-manipulator.

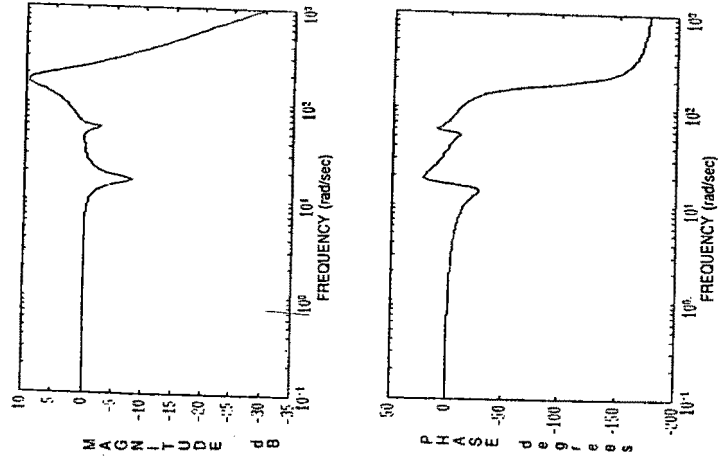


FIG. 5. Bode plot of force control ( $F_1/I$ ) on a macro/micro-manipulator.

manipulator exciting the macro-manipulator's structural dynamics (3). Clearly, in the limit, increasing  $M_2$  to infinity is equivalent to placing the micro-manipulator on the base, so there would be no structural dynamics to worry about. In fact, if the impedance of the macro-manipulator could be physically increased by a factor of 100, then the problem disappears (1). Since that is not a practical solution in this case, the next step is to determine whether it can be approximated through control action.

As described earlier, collocated positive force feedback tends to increase the apparent inertia. However, in order to achieve collocation, an actuator  $F_g$  must be placed between  $M_2$  and ground. Positive force feedback ( $F_g = +Gf$ ) would then increase the apparent end-point inertia, alleviating the anti-resonance problem (3). Again, this can actually be implemented using active local supports. It should be noted in passing that positive force feedback implemented on the base actuator ( $F = +Gf$ ) does not help much because the actuator and sensor are not collocated (3).

An alternative approach is to determine the cause of the exhibited anti-resonance and try to solve the problem at the root. Further examination of the macro/micro-manipulator model of Fig. 3 reveals why the macro-manipulator dynamics are excited. Since there is very little dissipation in the structure ( $B_2$  is very small), much of the energy transferred from the micro-manipulator to the macro-manipulator is reflected back through the structure, exciting structural modes. One way of alleviating this problem is by increasing the structural damping ( $B_2$ ). This is mechanically difficult to achieve, although not impossible (15). Another alternative is to increase  $B_2$  through control action. However, in order to achieve that, an actuator ( $F_c$ ) must be placed between  $M_1$  and  $M_2$ , with a control action:

$$F_c = -G(\ddot{X}_2 - \dot{X}_1).$$

The practicality of such an actuator, however, is unclear.

Another means of dissipating energy transferred by the micro-manipulator to the macro-manipulator is by increasing  $B_1$ . However, arbitrarily increasing  $B_1$  may not help. If  $B_1$  is increased to infinity,  $M_1$  becomes immobilized, and no energy is dissipated through  $B_1$ . There is, however, a value of  $B_1$  between zero and infinity that maximizes dissipation.

The bond graph of Fig. 3(b) has a structure similar to a lumped-parameter model of a transmission line (a chain of alternating I and C elements on 1 and 0 junctions respectively). If the macro-manipulator structure is viewed as a mechanical transmission line, where the micro-manipulator is the source input and  $B_1$  is the load, then the energy transferred from the source to the load can be maximized if the load's impedance is matched to the characteristic impedance of the transmission line (3). This is known as impedance matching (16).

The characteristic impedance of the macro-manipulator structure can be approximated (3) as:

$$Z_{11} = \sqrt{(M_1 + M_2)K}.$$

Thus, if we set the value of  $B_1$  equal to the characteristic impedance ( $Z_{11}$ ), most of

the energy transferred to the macro-manipulator structure could be dissipated through  $B_1$ , reducing the amount of reflection and hence excitation of structural modes (see Fig. 6).

The value of  $B_1$  can be modulated by actually placing a mechanical damper on the joint axis, or through control action. Modulating  $B_1$  through control action is easily achieved since there already exists an actuator ( $F$ ) between ground and  $M_1$ . The control law for the actuator would simply be:

$$F = -G\dot{X}_1.$$

Once the effect of the structural dynamics has been alleviated, the micro-manipulator can treat the macro-manipulator as a low-frequency disturbance, and high-bandwidth force control can be achieved through proportional feedback:

$$f = -GF_c.$$

Thus, a control action by the macro-manipulator of the form:

$$F = -G_1X_1 - G_2\dot{X}_1$$

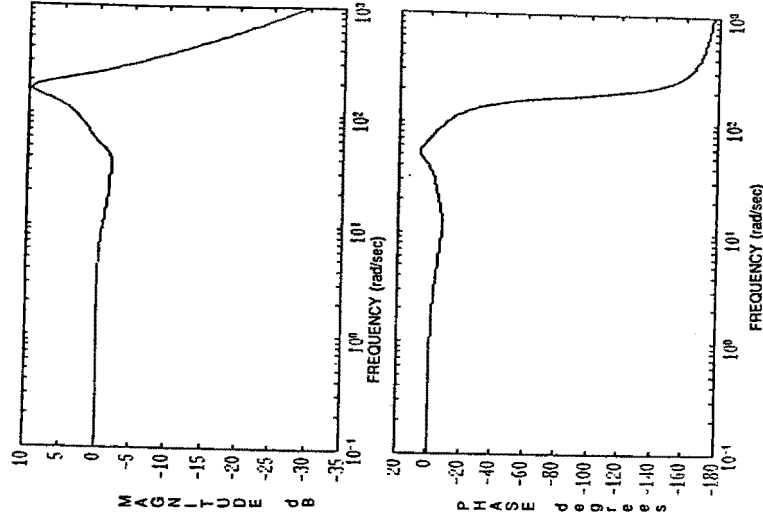


Fig. 6. Bode plot of force control ( $F_c/f$ ) on macro/micro-manipulator with  $B_1$  chosen through impedance matching.

along with a control action by the micro-manipulator of the form:

$$f = -G_3 F_1$$

is sufficient to achieve force regulation at bandwidths much higher than the fundamental structural frequency of the robot. The value of  $G_2$  is chosen based on impedance matching, while the values of  $G_1$  and  $G_3$  can be chosen using any of the common control techniques.

Once the proper physical architecture has been established, more elaborate controllers could be designed. However, in the experiments reported in the next section, this did not prove to be necessary.

It should be noted how throughout the design process the desired system behavior was approached by modifying elements of the physical system model such as actuator location, sensor location, values of masses, values of dampers, etc. Feedback was only introduced as a means of implementing some of these changes. Consequently, the proposed controller is very robust. We did not introduce a model-sensitive compensator, as did Tilley and Cannon (4), that would require a very accurate model of the system. Even if the velocity feedback around the base actuator is over or underestimated by as much as 50% from the correct value, the system remains well behaved.

#### K. Experimental Validation

To test the proposed controller design, an experimental one-axis macro/micro-manipulator test-bed was designed and constructed. The micro-manipulator described in Ref. (2) was attached to a very flexible (first structural mode at 1.8 Hz), one-axis macro-manipulator (see Fig. 7). The primary reason for using such a flexible structure was to accentuate the stability problems by examining an extreme case. The macro-manipulator was actuated at the base and could be controlled using either base measurements or end-point measurements relative to ground. The micro-manipulator was controlled using only end-point measurement. A number of experiments were performed in both end-point position and force control. In both cases, the achieved performance of the macro/micro-manipulator was compared to that of the macro-manipulator alone.

#### V.1. End-point position control

In this experiment it was desired to control the position of the system end-point. The micro-manipulator was controlled using end-point position and velocity feedback, while the macro-manipulator was controlled using base position and velocity feedback. A step position command was simultaneously issued to both the macro- and micro-manipulators. The response of the system end-point (micro-manipulator position) as well as that of the macro-manipulator is given in Fig. 8. It can be seen how the micro-manipulator reaches its target very quickly and locks in on it while the macro-manipulator is still moving. Recall that there was no connection between the micro-manipulator and ground. The micro-manipulator was carried by the macro-manipulator, yet it was capable of compensating for the macro-manipulator's undesirable motion.

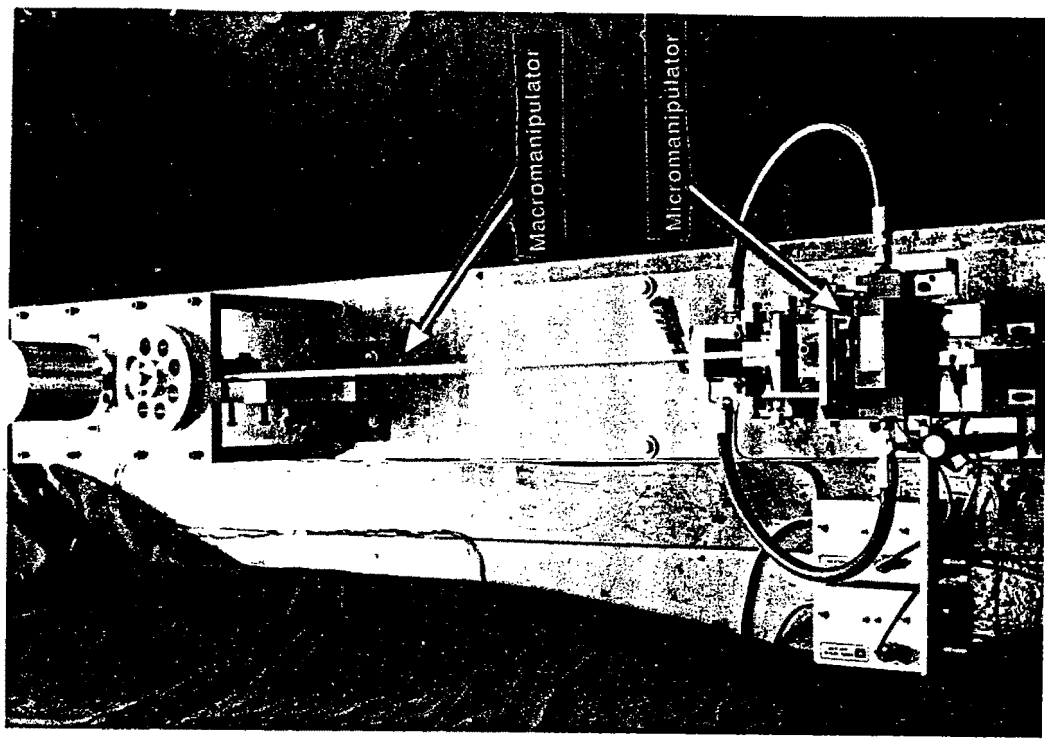


Fig. 7. Top-view photograph of experimental one-axis macro/micro-manipulator.



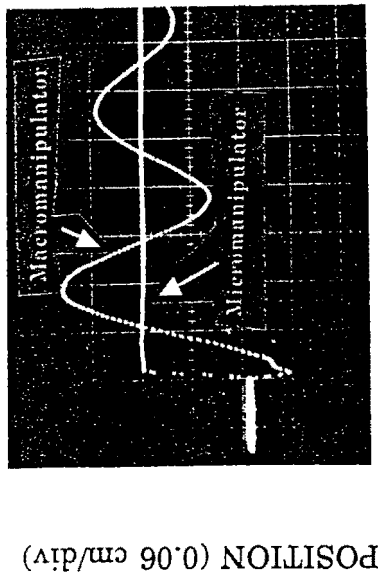


Fig. 8. Response of macro/micro-manipulator to a step position command.

The micro-manipulator was then issued a sinusoidal position command while the macro-manipulator was regulated about zero. Figure 9 illustrates the response of the system end-point versus input. At a frequency of 20 Hz the system tracks the input with no attenuation at all. A  $-3$  dB bandwidth of 28 Hz was achieved. This is more than an order of magnitude higher than the first structural mode (1.8 Hz), confirming that high-bandwidth end-point position control can be achieved by a simple, model-insensitive controller if the proper physical architecture is used.

#### V.2. High bandwidth force control

It was desired, in this experiment, to control the forces applied to an environment that is stiffer than the robot structure. Prior work has shown that the stiffness of the environment relative to the robot structure is of primary importance, and not necessarily the absolute stiffness. Specifically, using conventional robot architectures, it is extremely difficult to achieve good force control against environments that are as stiff or stiffer than the robot structure (7). Thus, an environment with a  $2631$  N/m (15 lb/in) stiffness (five times higher than the stiffness of the robot structure) was chosen. The applied force was measured with a piezo-electric force transducer attached to the system end-point.

With the micro-manipulator turned off, the macro-manipulator was commanded to apply a force of  $0.9$  N (0.2 lb) to the environment. The force measurement from the transducer was fed back in a negative proportional fashion to the base motor. The initial position of the macro-manipulator was  $0.13$  cm (0.050 in) away from the environment. Hence the system was out of contact with the environment at time zero. When the step force command was issued, the system impacted the environment and attempted to regulate the applied force. The force response at various gains is given in Fig. 10. It is observed that as the gain was increased,

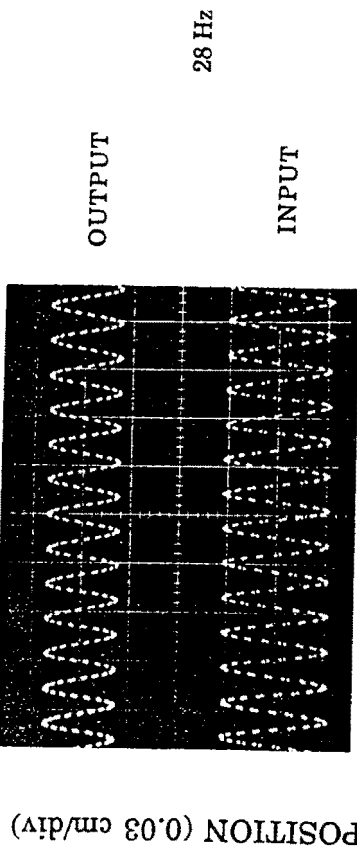
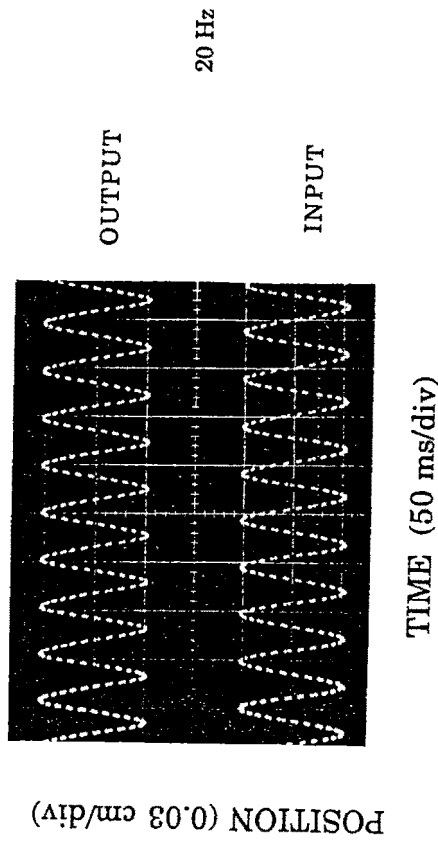


Fig. 9. Response of macro/micro-manipulator to sinusoidal position commands.

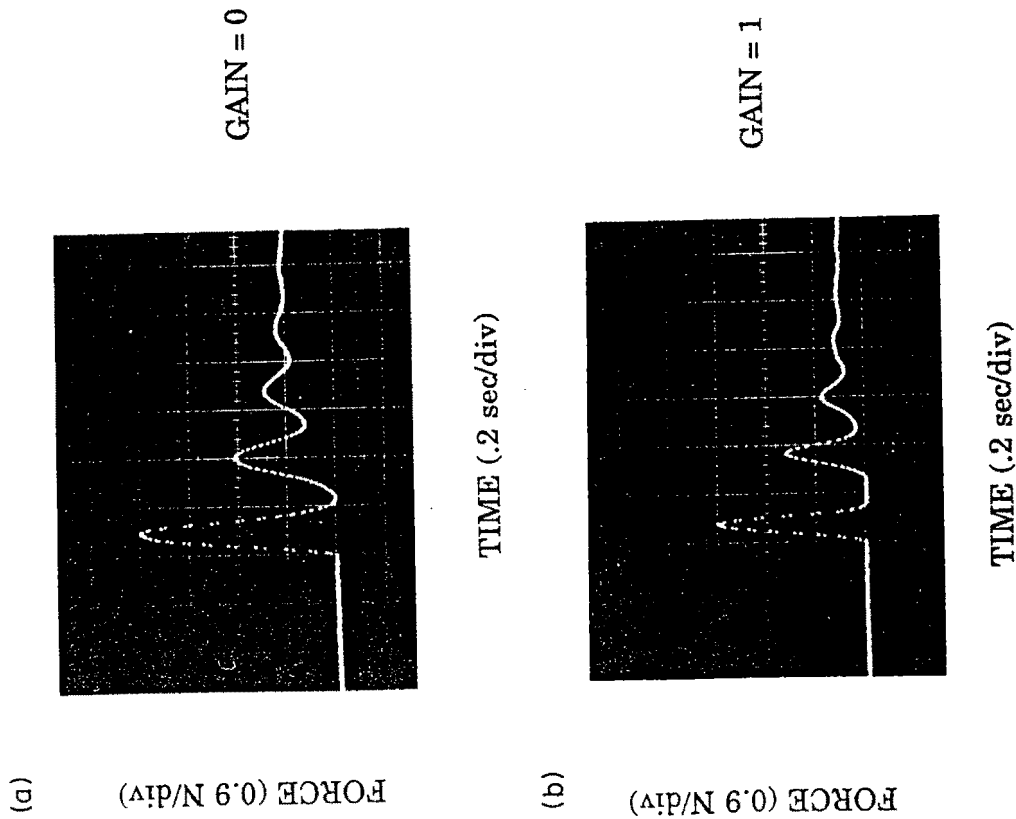


FIG. 10(a, b).

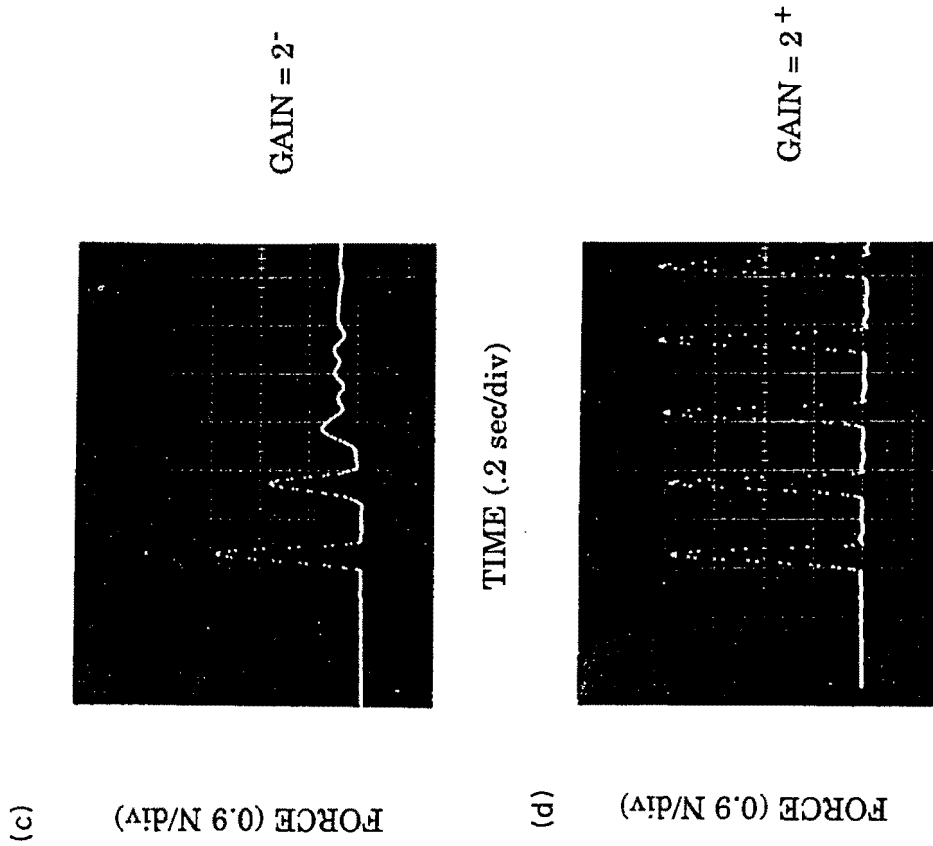


FIG. 10. Response of force-controlled macro-manipulator to a force step with initial impact.

bouncing became more severe. In fact, at a gain of about 2, the system became unstable. This confirms the analytical prediction that high performance force control on conventional robot architectures is inherently unstable due to non-collocation of actuator and sensor.

In the next experiment, the micro-manipulator was enabled and force was controlled by feeding back the measurement from the force transducer to the micro-manipulator in a negative proportional fashion. The macro-manipulator was controlled about zero using base position and velocity feedback. Once again, the system force step response is shown in Fig. 11(a). The best obtained force control response of the macro-manipulator alone (open loop) is repeated in Fig. 11(b) for comparison purposes. It is seen in Fig. 11(a) that the initial impact no longer produces a large force peak. Furthermore, the large oscillations exhibited by the macro-manipulator are greatly suppressed.

Figure 12 illustrates the macro/micro-manipulator's ability to track sinusoidal force commands. It is seen that up to a frequency of 50 Hz there is virtually no attenuation. A  $-3$  dB bandwidth of 60 Hz was achieved. This is 32 times higher than the first structural mode of the robot, demonstrating that high-bandwidth force control can be achieved by simple, model-insensitive controllers if the proper physical architecture is used.

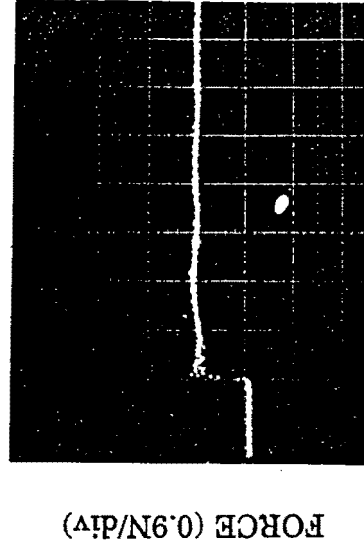
### 11. Conclusions

An approach to controller design in the physical domain was presented as a means of integrating control systems design with mechanical systems design. As a case study, the problem of high-performance position and force control of a robot was considered. Although the application of the method to this problem is *post hoc*, it was shown how this design approach may lead to alternative robot architectures that are inherently stable and well-suited for high-bandwidth end-point position and force control.

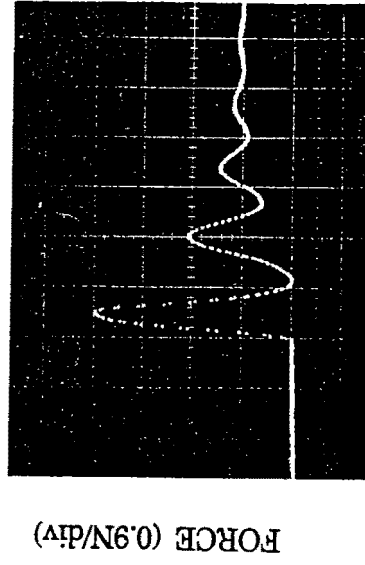
Experimental characterization of one of the proposed alternative robot architectures—the macro/micro-manipulator system—was also presented. It was shown to be inherently stable and well-suited for high-performance end-point control. Both end-point position and force control bandwidths considerably higher than the fundamental structural frequency of the robot were achieved.

The controllers considered here are simple, robust, and virtually model-insensitive. They were designed in the physical domain using simplified, inaccurate models. For example, the flexible beam used in this experiment is better characterized by a continuous model with an infinite number of modes. Yet, the work presented here used a lumped-parameter model of only one mode. Despite this fact, these controllers achieved the highest end-point position and force control performance levels reported to date (to the best of our knowledge) in the robotics literature.

On the other hand, conventional controller design methods have been refined to the point where detailed step-by-step procedures have been established. In the case-study of Controller Design in the Physical Domain presented in this paper, a great



TIME (.2 sec/div)  
(a)



TIME (.2 sec/div)  
(b)

Fig. 11. (a) Response of force-controlled macro/micro-manipulator to a force step with initial impact. (b) Response of open loop force-controlled macro-manipulator to a force step with initial impact.

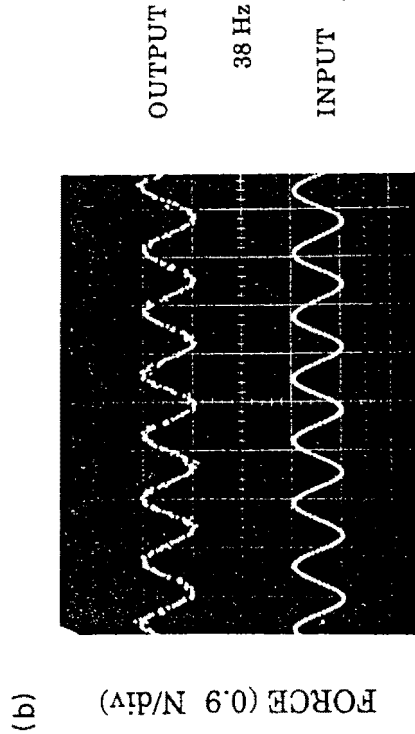
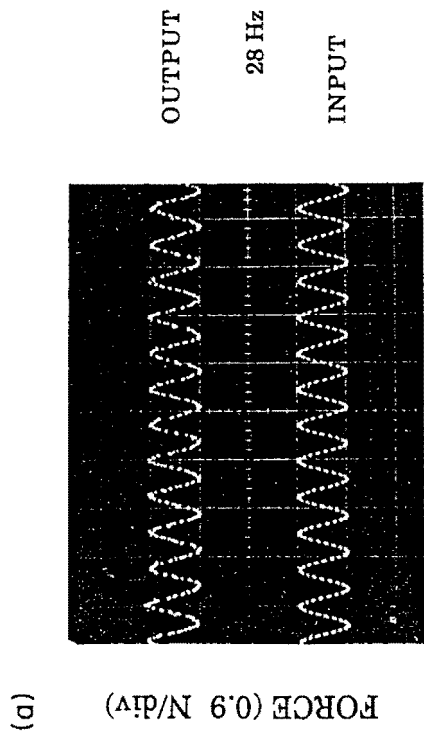


FIG. 12(a, b).

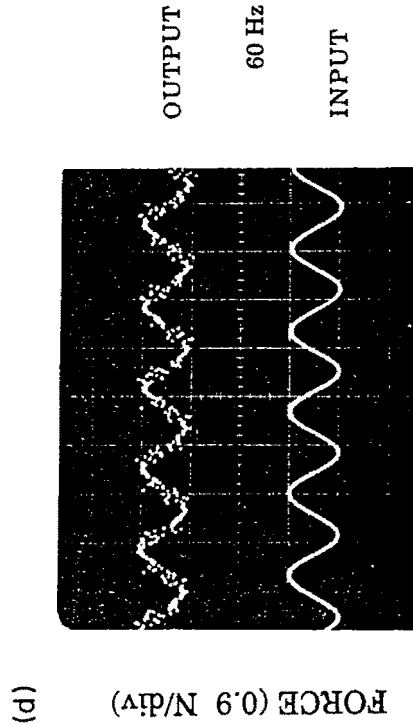
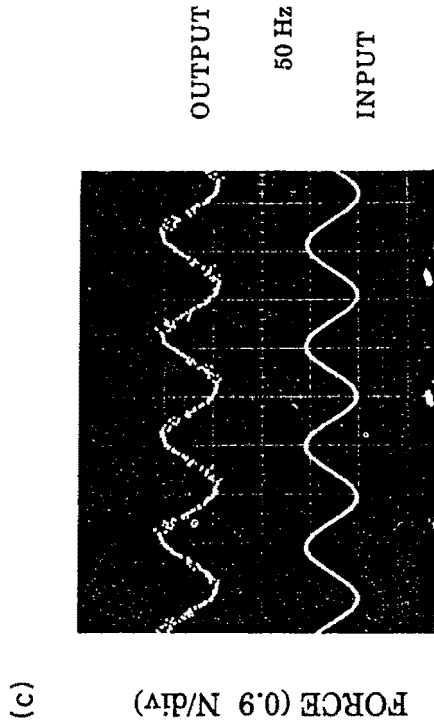


FIG. 12. Response of force-controlled macro/micro-manipulator to sinusoidal force commands.

deal of intuition based on past experience was used. The development of detailed methodology is a topic of ongoing and future research.

### References

- (1) A. Sharon, "The macro/micro manipulator: an improved architecture for robot control". Ph.D. Thesis, Department of Mechanical Engineering, Massachusetts Institute of Technology, 1989.
- (2) A. Sharon and D. E. Hardt, "Enhancement of a robot's accuracy using end-point feedback and a macro/micro manipulator system", Proceedings of the American Control Conference, June 1984.
- (3) A. Sharon, N. Hogan and D. E. Hardt, "High bandwidth force regulation and inertia reduction using a macro/micro manipulator system", Proceedings of the IEEE Conference on Robotics and Automation, 1988.
- (4) S. W. Tilley and R. H. Cannon, Jr., "Experiments on end-point position and force control of a flexible arm with a fast wrist", Proceedings of the AIAA Guidance and Control Conference, Aug. 1986.
- (5) N. Hogan, "Impedance control: an approach to manipulation: part I—Theory", *ASME J. Dynamic Syst. Measure. Control*, Vol. 107, Mar. 1985.
- (6) N. Hogan, "On the stability of manipulators performing contact tasks", *IEEE J. Robotics Automation*, Vol. 4, No. 6, Dec. 1988.
- (7) J. E. Colgate, "The control of dynamically interacting systems", Ph.D. Thesis, Department of Mechanical Engineering, Massachusetts Institute of Technology, 1988.
- (8) S. A. Schneider and R. H. Cannon, Jr., "Experiments in cooperative manipulation: a system perspective", NASA Conference on Space Telerobotics, Jan. 1989.
- (9) N. Hogan, "Stable execution of contact tasks using impedance control", Proceedings of the IEEE Conference on Robotics and Automation, Mar. 1987.
- (10) W. B. Gevarter, "Basic relations for control of flexible vehicles", *AIAA J.*, Vol. 8, No. 4, Apr. 1970.
- (11) R. H. Cannon, Jr. and E. Schmitz, "Initial experiments on the end-point control of a one link flexible experimental manipulator", *Int. J. Robotics Res.*, Vol. 3, No. 3, 1984.
- (12) S. D. Eppinger and W. P. Seering, "On dynamic models of robot force control", Proceedings of the IEEE Conference on Robotics and Automation, 1986.
- (13) W. J. Book, J. S. Le and V. Sangveraphunsiri, "The bracing strategy for robot operation", Theory and Practice of Robots and Manipulators, June, 1984.
- (14) H. Asada and H. West, "Design and analysis of braced manipulators for improved stiffness", 3rd International Symposium on Robotics Research, Oct. 1985.
- (15) T. Bailey and J. E. Hubbard, Jr., "Distributed piezoelectric-polymer active vibration control of a cantilever beam", *J. Guidance Control Dynamics*, Sept.-Oct. 1985.
- (16) G. Bekelci and A. H. Barrett, "Electromagnetic vibrations, waves, and radiation", M.I.T. Press, Cambridge, MA, 1977.

### Appendix

Transfer function relating endpoint position ( $X_{M_i}$ ) to actuator force ( $F$ ) of system in Fig. 1(a).

$$F = \frac{K}{S[M_1 M_2 S^3 + (B_1 M_2 + B_2 M_1)S^2 + (B_1 B_2 + K M_1 + K M_2)S + B_1 K]}$$

Equations of motion characterizing system in Fig. 1(b).

$$\frac{d}{dt} \begin{bmatrix} X_1 \\ \dot{X}_1 \\ X_2 \\ \dot{X}_2 \\ F_1 \end{bmatrix} = \begin{bmatrix} 0 & 1 & 0 & 0 & 0 \\ -\frac{K}{M_1} & -\frac{B_2 + B_1}{M_1} & \frac{K}{M_1} & \frac{B_2}{M_1} & 0 \\ 0 & 0 & 0 & 1 & 0 \\ \frac{K}{M_2} & \frac{B_2}{M_2} & \frac{K + K_1}{M_2} & \frac{B_2 + B_1}{M_2} & 0 \\ 0 & 0 & 0 & 0 & K_1 \end{bmatrix} \begin{bmatrix} X_1 \\ \dot{X}_1 \\ X_2 \\ \dot{X}_2 \\ F_1 \end{bmatrix} + \begin{bmatrix} 0 \\ 1 \\ M_1 \\ 0 \\ 0 \end{bmatrix} [F]$$

Equations of motion characterizing system in Fig. 3(b).

$$\frac{d}{dt} \begin{bmatrix} X_1 \\ \dot{X}_1 \\ X_2 \\ \dot{X}_2 \\ X_3 \\ \dot{X}_3 \\ F_1 \end{bmatrix} = \begin{bmatrix} 0 & 1 & 0 & 0 & 0 & 0 & 0 \\ -\frac{K}{M_1} & -\frac{B_2 + B_1}{M_1} & \frac{K}{M_1} & \frac{B_2}{M_1} & 0 & 0 & 0 \\ 0 & 0 & 0 & 1 & 0 & 0 & 0 \\ \frac{K}{M_2} & \frac{B_2}{M_2} & \frac{K}{M_2} & \frac{B_2 + B_1}{M_2} & 0 & B_3 & 0 \\ 0 & 0 & 0 & 0 & 0 & 0 & 1 \\ 0 & 0 & 0 & 0 & 0 & \frac{K_1}{M_3} & -\frac{B_1 + B_2}{M_3} \\ 0 & 0 & 0 & 0 & 0 & -\frac{M_2}{M_3} & 0 \end{bmatrix} \begin{bmatrix} X_1 \\ \dot{X}_1 \\ X_2 \\ \dot{X}_2 \\ X_3 \\ \dot{X}_3 \\ F_1 \end{bmatrix} + \begin{bmatrix} 0 \\ 1 \\ M_1 \\ 0 \\ 0 \\ 0 \\ 0 \end{bmatrix} [F]$$

$$\times \begin{bmatrix} X_1 \\ \dot{X}_1 \\ X_2 \\ \dot{X}_2 \\ X_3 \\ \dot{X}_3 \\ F_1 \end{bmatrix}$$